NASA TM X: 63178

COSMIC RAY DEUTERIUM AND HELIUM-3 OF SECONDARY ORIGIN AND THE RESIDUAL MODULATION OF COSMIC RAYS
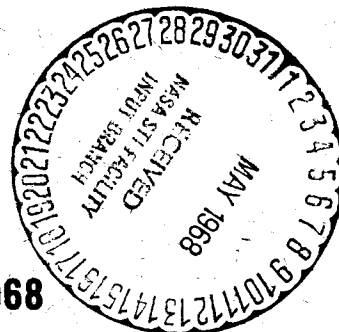
REUVEN RAMATY
RICHARD E. LINGENFELTER

APRIL 1968

GODDARD SPACE FLIGHT CENTER
GREENBELT, MARYLAND

COSMIC RAY DEUTERIUM AND HELIUM-3 OF SECONDARY ORIGIN AND THE RESIDUAL MODULATION OF COSMIC RAYS

Reuven Ramaty*
NASA-Goddard Space Flight Center, Greenbelt, Md.

Richard E. Lingenfelter**
Institute of Geophysics and Planetary Physics
University of California, Los Angeles, California

GODDARD SPACE FLIGHT CENTER
GREENBELT, MARYLAND

ABSTRACT

Assuming that cosmic ray deuterons and helium-3 nuclei are of secondary origin, we show that a unique determination of both the cosmic ray path length and the residual interplanetary field modulation at solar minimum may be made from a comparison of the calculated and measured intensities of these two nuclei. This determination does not depend on any assumptions regarding either the source spectra or the unmodulated proton-to-alpha particle ratio of the primary cosmic rays. The production of deuterium and helium-3 by cosmic ray interactions in the galaxy is calculated, considering energy-dependent cross-sections, interaction kinematics and demodulated cosmic ray spectra. The resulting flux at the earth is obtained by taking into account leakage from the galaxy, ionization losses, nuclear breakup and modulation. From a comparison of these calculations with the measured deuterium and helium-3 intensities at the earth, we conclude that within the experimental uncertainties all the data can be understood in terms of an energy-independent cosmic ray path-length of 4 ± 1 g/cm^2 and a residual interplanetary field modulation at solar minimum which above 600 MV is of the form $\exp(-\eta/R\beta)$ with $\eta = 0.35 \pm 0.15$ BV, where R and β are rigidity and velocity respectively.

COSMIC RAY DEUTERIUM AND HELIUM-3 OF SECONDARY ORIGIN

AND THE RESIDUAL MODULATION OF COSMIC RAYS

I. INTRODUCTION

The abundance of deuterium and helium-3 in the cosmic rays was found to be significantly larger than that expected from the study of the universal abundance of elements. It has been suggested, therefore, that these isotopes are of secondary origin, produced by nuclear interactions of cosmic rays with the interstellar gas and that the comparison of the observed and calculated intensities of deuterium and helium-3 could determine the mean amount of material traversed by cosmic rays in interstellar space.

Previous studies of d and He^3 production were made by Hayakawa et al (1958), Foster and Mulvey (1963), Badhwar and Daniel (1963), Dahanayake et al (1964), Kuzhevskii (1966), Fichtel and Reames (1966), Badhwar and Kaplon (1966), Biswas et al (1966), Meyer et al (1968), and Biswas et al (1968). The mean cosmic ray path lengths deduced from these studies range from a few g/cm^2 to more than 10 g/cm^2 and they may or may not be energy dependent. Even though these values are of the same order as the path length deduced from the observed abundances of Li, Be and B (Shapiro and Silberberg, 1968), the

determination of the amount of material traversed by cosmic
rays at low energies is seriously complicated by an unknown
residual solar modulation.

The existance of such a residual modulation, active even
at solar minimum, is indicated by the measurements of an inter-
planetary gradient, between the orbits of the earth and Mars,
in the proton and alpha particle fluxes (O'Gallagher and Simpson,
1967; O'Gallagher, 1967). The measurement of this gradient,
however, determines only the relative modulation over a distance
of roughly an astronomical unit, and not the total residual mod-
ulation, which short of direct measurements over large distances
in the solar system, remains essentially undetermined.

In a preliminary report of rather extensive calculations
of deuterium and helium-3 production (Ramaty and Lingenfelter,
1968), we suggested that because of the secondary origin of these
nuclei and because of their different charge-to-mass ratio, a
comparative study of d and He^3 in the cosmic rays allows an es-
sentially independent determination of both the amount of ma-
terial traversed by cosmic rays and their total residual modu-
lation in the interplanetary magnetic field. Unlike previous
attempts to estimate the total modulation, this technique re-
lies solely on the assumption that the observed d and He^3 are
of secondary origin, and does not depend on any arbitrary assump-
tion about the charge ratios or spectral shapes of the primary
cosmic rays either in interstellar space or at their sources.

In the present paper we give a detailed discussion of these calculations and conclusions.

The production spectra of deuterium and helium-3, resulting from the interaction of cosmic ray protons, alpha-particles and medium nuclei with the interstellar gas, are calculated by taking into account the energy dependence of the cross-sections, the kinematics and the secondary energy distributions of the various d and He^3 producing interactions. Using these spectra, the equilibrium d and He^3 fluxes are evaluated by considering leakage from the galaxy, ionization losses and nuclear breakup. The residual solar modulation is taken into account by first demodulating the observed primary cosmic ray fluxes at the earth, thenby using these demodulated intensities to calculate the production of d and He^3 in interstellar space and finally by modulating the resultant secondary equilibrium fluxes with the same modulating function as used in the initial demodulation process. By comparing the resultant d and He^3 spectra with the observations, it is demonstrated that the measured deuteron and helium-3 fluxes at the earth can be best understood in terms of an energy-independent path length and a residual solar modulation which is both velocity and rigidity dependent.

II. DEUTERON AND HELIUM-3 PRODUCTION

The rate of production of secondary nuclei by cosmic ray interactions in the interstellar material may be written as

$$q_s(E_s) = 4\pi \sum_i \int dE \, j_i(E) \, n_i \, \sigma_i(E) \, F_i(E, E_s) \tag{1}$$

where q_s is the production spectrum of secondary nuclei per second per gram of interstellar material; E and E_s are the energies per nucleon of the primary and secondary particles respectively; j is the equilibrium intensity in interstellar space of the interacting cosmic ray nuclei; n is the number of target nuclei per gram of interstellar material; σ is the inter-action cross-section; and $F(E, E_s)dE_s$ is the probability that a primary cosmic ray nucleus of energy per nucleon E will produce a secondary nucleus of energy per nucleon in dE_s around E_s.

The production is summed over all interactions, i, which produce the secondary nucleus, s. The interactions which we have considered for the production of deuterium, helium-3 and tritium, which decays into helium-3, are listed in Table 1. Each of these interactions may also include the generation of pions.

The interstellar material is assumed to be composed of hydrogen, helium and CNO nuclei in the ratio $1:10^{-1}:10^{-3}$ (Suess and Urey, 1956; Cameron, 1959)

We shall now provide detailed discussions of the primary cosmic ray intensities, production cross-sections, and the

kinematics and secondary energy spectra to be used in the evaluation of equation (1).

Primary Cosmic Ray Intensities

The energy spectra of the various charge components of the primary cosmic radiation were measured near the earth at solar minimum by Freier and Waddington (1965), Balasubrahmanyan et al (1966 a,b), Comstock et al (1966), Fan et al (1966b), Hofmann and Winckler (1966), Ormes and Webber (1966) and Waddington and Freier (1966). The interstellar primary cosmic ray intensities used to evaluate equation (1) are obtained by demodulating these measured spectra with a modulating function, M , of the form $\exp(-\eta/\beta f(R))$, based on Parker's (1958) solar wind model. The modulating parameter η , which is space and time dependent, defines the total residual solar modulation, β is the particle velocity in units of c , and f(R) is a function of magnetic rigidity and depends on the distribution of the interplanetary magnetic field irregularities. It was first suggested by Dorman (1963) that f(R) could be approximated by $f(R)=R_0$ for $R<R_0$ and $f(R)=R$ for $R>R_0$, where R_0 is a characteristic transition rigidity depending on the distribution of the magnetic irregularities. Subsequently, Jokipii(1966,1968) and Jokipii and Coleman (1968) demonstrated that such a form is consistent with the measured power spectrum of the interplanetary field variations, with R_0 essentially time dependent and of the order of several

hundred MV in 1965. With this functional form for f(R), the modulating function mentioned above can be written as

$$M = \begin{matrix} \exp\left(-\eta / R_0 \beta\right) & , & R < R_0 \\ \exp\left(-\eta / R \beta\right) & , & R > R_0 \end{matrix} \qquad (2)$$

Gloeckler and Jokipii (1966), Balasubrahmanyan et al (1967), O'Gallagher and Simpson (1967) and O'Gallagher (1967) have also shown that the measured temporal and spatial variations of cosmic rays in the interplanetary medium can be explained by such a modulation, but have deduced different values for the modulating parameter R_0. Since there is no general agreement as to the value of R_0, and since the modulating parameters which define the total modulation may be different from the values obtained from the temporal and spatial variations mentioned above, we have treated both η and R_0 as free parameters to be determined from the present study.

Production Cross-Sections

The deuteron production cross-section for proton-proton interactions has been measured in considerable detail from threshold to a few Bev by Schulz (1952), Crawford (1953), Stevenson (1953), Durbin et al. (1951), Fields et al. (1954), Stadler (1954), Baldoni et al (1962), Guzhavin et al (1964), Neganov and Parfenov (1958), Chapman et al (1964), Fickinger et al (1962), Pickup et al (1962), Smith et al (1961) and Hart et al (1962), and the theory of the interaction has been studied by Rosenfeld (1954). This cross-section data together with a

smoothed curve used in the present calculation are shown in Figure 1.

The cross-sections for the production of deuterons, tritons and helium-3 nuclei from the breakup of He^4 were measured in proton interactions with alpha particles at 28 Mev by Wickersham (1957), at 31 Mev by Bunch et al (1964), at 32 Mev by Benveniste and Cork (1953), at 53 Mev by Cairns et al (1964), at 55 Mev by Hayakawa et al (1964), and at 95 Mev by Selove and Teem (1958), and in neutron interactions with alpha particles at 90 Mev by Tannenwald (1953), and at 300 Mev by Moulthrop (1955) and Innes (1957). These data are shown in Figure 2. We have assumed that the He^4 breakup cross-sections at these energies are the same for incident protons as for neutrons. The measurement of the pickup cross-section by Tannenwald (1953) of 12 ± 2.5 mb for 90 Mev neutrons in the reaction $n\alpha \rightarrow dt$ and by Selove and Teem (1958) of 15 ± 3 mb for 95 Mev in the reaction $p\alpha \rightarrow dHe^3$ suggest that the coulomb barrier for protons is not important at these energies and that these cross-sections are equal. At lower energies, particularly near the threshold, the coulomb barrier is important and the proton pickup cross-section is much lower than that for neutrons, which shows a resonance at about 22.15 Mev.

Measurements of alpha particle breakup were also made at 630 Mev by Kozadaev et al. (1960) and at 970 Mev by Riddiford

and Williams (1960). These measurements differentiate between reactions having two, three or more charge particles in the final state but do not completely distinguish between the various modes. Therefore, some assumptions must be made in order to obtain the deuteron, triton and helium-3 yields. It was shown by Moulthrop (1955) and Innes (1957) that in 3-prong reactions (three charged particles in the final state) the ratios between the alpha particle breakup modes into singly charged fragments, pt:pnd:dd:2p2n $\approx$ 0.58:0.26:0.12:0.04, are the same in both pion and non-pion producing reactions and that these rates are roughly independent of energy.

Using this relationship, and the fact that Kozadaev et al (1960) did measure the non-pionic pt breakup, we can separate their 3-prong cross-section into partial cross-sections for these breakup modes for both pion and non-pion producing reactions. A similar treatment is applied to the data of Riddiford and Williams (1960) with the additional assumption that π^0 and π^+ production are roughly equal.

In order to reduce the 2-prong inelastic reactions which include the dHe^3 and $pnHe^3$ final states, we make three assumptions: (a) pion production without alpha particle breakup constitutes roughly 10% of the total pion production cross-section at energies greater than 300 Mev, based on the measurements of Innes (1957); (b) π^+ and π^0 production are roughly equal; and (c) the dHe^3 and $pnHe^3$ final states are equally probable in pion

producing reactions, based on a similar equality found for non-pionic modes in the lower energy measurements. The cross-sections thus deduced are shown in parentheses in Figure 2, together with the inferred energy-dependent partial cross-section for $p\alpha$ interactions.

In the absence of data on helium-4 breakup in $\alpha\alpha$ interactions, we have assumed that the same breakup modes occur and that their cross-sections are simply four times those in αp interactions at the same available kinetic energy in the center of mass frame. Since our calculations suggest that $\alpha\alpha$ interactions make a non-negligible contribution to d and He^3 production, a measurement of the breakup cross-sections in the energy range around 100 Mev would be particularly valuable.

The deuteron production cross-section in proton interactions with CNO nuclei was measured at 18.5 Mev by Nadi and Riad (1964), at 20 Mev by Legg (1963), at 40 Mev by Kavaloski et al (1963) and at 190 Mev by Bailey (1956). At higher energies the cross-section can be estimated from the d/t yields calculated by Fraenkel (personal communication) and measured by Schwarzschild and Zupancic (1963). The tritium production cross-section for these interactions was measured at 43 Mev by Cherny and Pehl (personal communication), at 150 Mev by Brun et al (1962), at 190 Mev by Bailey (1956), at 224, 300, 400 and 750 Mev by Honda and Lal (1960), at 450 Mev and 2.05 Bev by Currie et al (1956), at 2.2 Bev by Fireman and Rowland (1955), and at 6.2 Bev by Currie

(1959). The helium-3 production cross-section in proton-CNO

interactions is not well measured, but the measurements of

Bailey (1956) at 190 Mev and the Monte Carlo calculations of

Fraenkel (personal communication) indicate that the He^3/H^3

yields are of the order of 1.7 from protons of energies be-

tween a hundred and several hundred Mev, and we have assumed

that this ratio holds for all energies. These cross-sections,

averaged to a mean value for CNO in the cosmic-ray nuclear

ratio of 0.45:0.10:0.45 (Comstock et al, 1966) are shown in

Figure 3.

Kinematics and Secondary Energy Spectra

The distribution functions $F(E,E_s)$ can be determined

from measurements of the angular and energy distributions of

deuterons and helium-3 nuclei produced in nuclear interactions.

Consider the interaction of an incident particle of mass m_i

and Lorentz factor, $\gamma = 1 + E/m_i$, with a stationary target

nucleus of mass m_t. Such a reaction may produce two or more

secondary particles. Consider one of these particles and let

$P(\gamma, \gamma_s^*, \cos\theta^*)\, d\gamma_s^*\, d\cos\theta^*$ be the probability that in the center

of mass frame it is emitted into $d\cos\theta^*$ around $\cos\theta^*$ with

Lorentz factor in $d\gamma_s^*$ around γ_s^*. In terms of this pro-

bability, the distribution function $F(\gamma, \gamma_s)$ may be written

as

$$F(\gamma, \gamma_s) = \int d\gamma_s^*\, P(\gamma, \gamma_s^*, \cos\theta^*)\, \frac{d\cos\theta^*}{d\gamma_s} \qquad (3)$$

The laboratory Lorentz factor γ_s is determined from the center of mass Lorentz factor and emission angle by

$$\gamma_s = \gamma_c \gamma_s^* + \sqrt{\gamma_c^2 - 1} \sqrt{\gamma_s^{*2} - 1} \cos\theta^* \qquad (4)$$

where γ_c is the Lorentz factor of the center of mass

$$\gamma_c = \frac{\gamma m_i + m_t}{E'} = \frac{E'^2 + m_t^2 - m_i^2}{2 m_t E'} \qquad (5)$$

and E' is the total available energy in the center of mass frame

$$E' = \sqrt{m_i^2 + m_t^2 + 2\gamma m_i m_t} \qquad (6)$$

Substituting $d\cos\theta^* / d\gamma_s$ from equation (4) into equation (3), we get

$$F(\gamma, \gamma_s) = \frac{1}{\sqrt{\gamma_c^2 - 1}} \int d\gamma_s^* \frac{P(\gamma, \gamma_s^*, \cos\theta^*)}{\sqrt{\gamma_s^{*2} - 1}} \qquad (7)$$

If the final state consists of more than two particles, the Lorentz factor, γ_s^*, of one of the secondary particles having mass m_s may have any value up to a maximum which is determined by the conservation of momentum and energy and is given by

$$\gamma_m^* = \frac{E'^2 + m_s^2 - m_r^2}{2 m_s E'} \qquad (8)$$

where m_r is the sum of the masses of all the other secondary

particles. However, if the final state consists of only two
particles, $\gamma_s^* = \gamma_m^*$, and the probability distribution $P(\gamma, \gamma_s^*, \cos\theta^*)$
reduces to a delta function in γ_s^* and equation (7) becomes

$$F(\gamma, \gamma_s) = \frac{P(\gamma, \cos\theta^*)}{\sqrt{\gamma_c^2 - 1}\,\sqrt{\gamma_m^{*2} - 1}} \tag{9}$$

For the purpose of evaluating the integrals over γ and γ_s^*
given in equations (1) and (3), we have to consider the ranges
of the incident Lorentz factor γ and the secondary Lorentz fac-
tor γ_s^* which can contribute to a given laboratory Lorentz fac-
tor γ_s . Since γ_c is uniquely determined by γ and vice versa,
the permissible range of γ_c also determines that of γ . These
ranges are determined by the requirements that $|\cos\theta^*| \leq 1$,
and that $\gamma_s^* \leq \gamma_m^*$ for more than two particles, or $\gamma_s^* = \gamma_m^*$
for only two particles in the final state respectively.

Using equation (4), the restrictions on $\cos\theta^*$ imply that

$$-1 \leq \frac{\gamma_s - \gamma_c \gamma_s^*}{\sqrt{\gamma_c^2 - 1}\,\sqrt{\gamma_s^{*2} - 1}} \leq 1 \tag{10}$$

For a fixed γ_s, this inequality restricts γ_c and γ_s^* to
the inside of a hyperbola given by

$$\gamma_c^2 + \gamma_s^{*2} + \gamma_s^2 - 2\gamma_c \gamma_s^* \gamma_s - 1 = 0 \tag{11}$$

For illustration, such hyperbolae are shown by solid lines in
Figure 4 for γ_s = 1.01, 1.1 and 2.0, corresponding to deuterons
of roughly 10, 100 and 1000 Mev/nucleon respectively. The three
branches of each hyperbola are separated by the points $(\gamma_c = \gamma_s; \gamma_s^* = 1)$
and $(\gamma_c = 1; \gamma_s^* = \gamma_s)$. The value of $\cos\theta^*$ equals -1 on the

two branches which extend out to large values of γ_c and γ_s^*, and $\cos\theta^* = +1$ on the remaining branch. Inside of each hyperbola $\cos\theta^*$ has values between +1 and -1.

The dashed curves in figure (4) are plots of γ_m^* as a function of γ_c, determined from equations (5) and (8) for the reactions $H^1(p,d)\pi^+$, $He^4(p,d)He^3$ and $p(He^4,d)He^3$. At threshold $\gamma_m^* = 1$ and $\gamma_c = \gamma_{ct}$, which is the Lorentz factor of the center of mass at threshold. Since at threshold $E' = m_s + m_r$, from equation (5) we obtain

$$\gamma_{ct} = \frac{(m_s + m_r)^2 + m_t^2 - m_i^2}{2 m_t (m_s + m_r)}$$

(12)

As the incident energy increases above threshold, γ_c and γ_m^* also increase above their threshold values and γ_m^* may or may not become greater than γ_c. The condition for this may be seen from the asymptotic behavior of γ_m^* at large incident energies, $\gamma_m^* \sim \frac{m_t}{m_s}\gamma_c$. Thus if $m_t > m_s$, for $\gamma_c > \gamma_{c2}$, $\gamma_m^* > \gamma_c$, where γ_{c2} is the value of γ_c at which $\gamma_m^* = \gamma_c$. The value of γ_{c2} can be directly evaluated from equations (5) and (8) and is given by

$$\gamma_{c2} = \frac{(m_s^2 - m_r^2) - (m_t^2 - m_i^2)}{2\sqrt{(m_s - m_t)[m_t(m_s^2 - m_r^2) - m_s(m_t^2 - m_i^2)]}}$$

(13)

For values of γ_c greater than γ_{c2}, secondary particles may be emitted in the laboratory frame into both the forward and backward cones. When γ_s^* equals γ_c, particles emitted with $\theta^* = -\pi$ in the center of mass frame, have zero kinetic energy

in the laboratory frame. However, if $m_t < m_s$, γ_m^* can never

equal γ_c and in the laboratory frame, the secondary particle

will always be emitted into the forward cone with nonvanishing

energy.

The lower limit, $\gamma_{c\ell}$, of the range of values of γ_c which

may contribute to a given γ_s is determined by the first inter-

section of γ_m^* with the hyperbola corresponding to the given γ_s,

as can be seen in figure 4. Depending on whether $\gamma_s > \gamma_{ct}$ or

$\gamma_s < \gamma_{ct}$, this corresponds to particles being emitted in the

center of mass frame into the forward or backward directions.

The upper limit on γ_c, however, is not necessarily finite.

The asymptotic forms of the two branches of the hyperbola cor-

responding to a given γ_s are $\gamma_c \left[\gamma_s \pm \sqrt{\gamma_s^2 - 1} \right]$ and, as men-

tioned above, for large γ_c, $\gamma_m^* \sim (m_t/m_s)\gamma_c$. There-

fore, if

$$ \gamma_s - \sqrt{\gamma_s^2 - 1} \; < \; \frac{m_t}{m_s} \; < \; \gamma_s + \sqrt{\gamma_s^2 - 1} \tag{14} $$

γ_m^* will remain always inside the hyperbola corresponding to

γ_s. This inequality is equivalent to $\gamma_s > \gamma_s(\infty)$, where $\gamma_s(\infty)$

is equal to $\frac{1}{2}(m_t/m_s + m_s/m_t)$ and at large incident energies $\gamma_s(\infty)$

is the asymptotic value of the Lorentz factor of secondary par-

ticles, γ_s, emitted in the backward direction in the center of

mass frame. Because of the relativistic addition of velocities,

$\gamma_s(\infty)$ is independent of the incident energy and therefore pro-

jectiles of the greatest energies may always produce secondary

particles with $\gamma_s > \gamma_s(\infty)$, provided they are emitted close enough to the backward direction in the center of mass frame. In these cases, the upper limit, γ_{cu}, becomes infinite.

When $\gamma_s < \gamma_s(\infty)$ we have to consider separately the cases in which $m_t > m_s$ or $m_t < m_s$. For $m_t > m_s$ and two particles in the final state, the upper limit γ_{cu} is determined by the second intersection of γ_m^* and the hyperbola corresponding to γ_s. If there are more than two particles in the final state, however, γ_{cu} becomes infinite. On the other hand, for $m_t < m_s$, γ_{cu} is determined by the second intersection of γ_m^* with the hyperbola corresponding to γ_s, regardless of the number of particles in the final state.

Finally, a further distinction exists between reactions having m_t greater or smaller than m_s, namely that for $m_t > m_s$, the curve γ_m^* will intersect every hyperbola at least once, whereas for $m_t < m_s$, γ_s has to be greater than a minimal value, $\gamma_s(min)$, in order that the corresponding hyperbola be intersected by γ_m^*. This can be seen by composing the curves of γ_m^* for the reactions $He^4(p,d)He^3$ and $p(He^4,d)He^3$ in Figure (4). This minimal laboratory Lorentz factor is obtained when $\gamma_s^* = \gamma_m^*$, and the secondary particle is emitted into the backward direction in the center of mass frame, $\theta^* = -\pi$.

From equation (4) with $\gamma_s{}^* = \gamma_m{}^*$ and $\theta^* = -\pi$, we find that the derivative of γ_s vanishes when

$$\left(\frac{\gamma_c}{\sqrt{\gamma_c^2-1}} - \frac{\gamma_m^*}{\sqrt{\gamma_m^{*2}-1}} \right) \left(\frac{d\gamma_m^*}{d\gamma_c} - \frac{\sqrt{\gamma_m^{*2}-1}}{\sqrt{\gamma_c^2-1}} \right) = 0 \qquad (15)$$

The first term will never vanish since $\gamma_m{}^* < \gamma_c$; the laboratory Lorentz factor γ_s will go through a minimum when the second term vanishes. The values of γ_c and $\gamma_m{}^*$ which satisfy equation (15), γ_c (min) and $\gamma_m{}^*$ (min), are obtained from equations (5) and (8) and are given by

$$\gamma_c(\text{min}) = \frac{m_i(m_s^2 + m_t^2 - m_i^2 - m_r^2) - 2m_r(m_t^2 - m_i^2)}{2m_t \sqrt{m_i(m_s^2 - m_r^2) - m_r(m_t^2 - m_i^2)}} \qquad (16)$$

and

$$\gamma_m^*(\text{min}) = \frac{m_r(m_t^2 + m_r^2 - m_s^2 - m_i^2) + 2m_i(m_s^2 - m_r^2)}{2m_s \sqrt{m_i(m_s^2 - m_r^2) - m_r(m_t^2 - m_i^2)}} \qquad (17)$$

The incident kinetic energies per nucleon E_{th}, E_z, E_{min} corresponding to γ_{ct}, γ_{cz} and γ_c(min), as well as the secondary laboratory kinetic energies per nucleon E_s(th), E_s(min) and $E_s(\infty)$, corresponding to γ_{ct}, γ_s(min) and $\gamma_s(\infty)$ are shown in Table 2. (Note that at threshold $\gamma_s = \gamma_c = \gamma_{ct}$).

- 17 -

For illustration, the range of possible secondary energies as a function of incident energy is shown in figure (5) for a variety of deuteron-producing reactions. The curves represent the kinematic limits determined from equation (4) for $\cos\theta^* = \pm 1$ and form the envelope of permissible secondary energies corresponding to intermediate values of $\cos\theta^*$. The significance of the various minima and asymptotic limits listed in Table 2 may also be seen in figure (5).

The center of mass angular distribution of deuterons from the reaction $H(p,d)\pi^+$ was well measured and has been studied by Rosenfeld (1954) who showed that the $(\frac{3}{2}, \frac{3}{2})$ interaction was dominant and that the distribution was therefore given by $\frac{1}{3} + \cos^2\theta^*$. Since this reaction also results in two bodies in the final state, the deuteron distribution function is then given directly from the angular distribution and equation (9).

$$F(\gamma, \gamma_s) = \frac{1/3 + \cos^2\theta^*}{\sqrt{\gamma_c^2 - 1}\,\sqrt{\gamma_m^{*2} - 1}} \tag{18}$$

The center of mass angular distribution of deuterons from the reaction $He^4(p,d)He^3$ was measured at 31 Mev by Bunch et al. (1964), at 55 Mev by Hayakawa et al. (1964), and at 95 Mev by Selove and Teem (1958). These measurements are shown in figure (6) and they can be fitted in detail by the model of Smith

and Ivash (1962) based on the distorted wave Born approxi-
mation with diffuse-well nuclear optical potentials. For
the purposes of this calculation, however, we have fitted
the distributions by functions of the form:

$$P(\gamma, \cos\theta^*) = \frac{\exp[-(1-\varepsilon\cos\theta^*)/\cos\theta_0]}{\cos\theta_0[1 - \exp(-2/\cos\theta_0)]} \tag{19}$$

where $\cos\theta_0$ depends on the incident Lorentz factor γ. In
the incident energy region of 30 to 90 Mev/nucleon, $\cos\theta_0$
can be well fitted by

$$\cos\theta_0 = \exp[9.38(\gamma-1)] \tag{20}$$

and we assumed this energy dependence for all values of γ
considered.

Since this reaction results in two bodies in the final
state, the distribution function $F(\gamma, \gamma_s)$ for both deuterons
and helium-3 nuclei is determined from equations (9) and (19).
The parameter ε is $+1$ in the reactions $He^4(p,d)He^3$ and
$H^1(\alpha, He^3)d$ and is -1 in the reactions $H^1(\alpha, d)He^3$ and
$He^4(p,He^3)d$.

Above the pion production threshold the more complex
reactions leading to $dHe^3\pi^0$ and $dt\pi^+$ also become signifi-
cant, as can be seen from the cross-sections shown in figure(2).

It has been shown by Riddiford and Williams (1960), however, that pions produced in proton-helium reactions are ejected as from the collision of free nucleons. Because of this, we have assumed that, kinematically, the $dHe^3\pi^o$ and $dt\pi^+$ reactions are similar to the reaction $H(p, d)\pi^+$, and therefore the distribution functions $F(\gamma, \gamma_s)$ are given by equation (18), where γ_c and γ_m^* are determined by equations (5) and (8) with $m_i = m_t = m_p$, $m_s = m_d$ and $m_r = m_\pi$.

The energy spectra in the laboratory frame of deuterons from pnd breakup of He^4 and of tritons from pt breakup of He^4 were measured by Tannenwald (1953) and by Innes (1957) for incident neutrons of 90 and 300 Mev, respectively. These data are shown in figure (7), normalized to a unit integral. As can be seen, within the experimental uncertainties, the triton spectrum from the multibody pt breakup of He^4 is independent of the incident neutron energy and can be fitted by a simple exponential of the form: $\exp\left(-E_t/E_o\right)$ where E_t is the triton kinetic energy per nucleon and $1/E_o$ is equal to 0.27 (Mev/nucleon)$^{-1}$. Similarly, the deuteron spectrum may be fitted by an exponential with $1/E_o = 0.063$ (Mev/nucleon)$^{-1}$.

These spectra indicate that in the laboratory frame the multinucleon fragments tend to be produced predominantly with low energies. This will happen if the angular and Lorentz-factor distributions in the center of mass are peaked in

the backward direction and around Lorentz factors which are about equal to the Lorentz factor of the center of mass. Assuming that the characteristic energy, E_0, is independent of the incident energy, the exponential distribution in kinetic energy per nucleon may be transformed into an exponential distribution in the center of mass angle, Θ^* . We assumed, therefore, that for the multibody reactions, $He^4(p,p')npd,dd,pt$ and nHe^3, the probability distribution function $P(\gamma, \gamma_s^*, \cos\Theta^*)$ is given by

$$P(\gamma, \gamma_s^*, \cos\Theta^*) = \frac{\exp\left[-(1-\varepsilon\cos\Theta^*)/\cos\Theta_0\right]}{\cos\Theta_0\left[1-\exp(-2/\cos\Theta_0)\right]} \delta(\gamma_s^* - \bar{\gamma}_s^*) \quad (21)$$

where in $p\alpha$ interactions, the parameter ε equals -1 and $\bar{\gamma}_s^* = \gamma_m^*$ for $\gamma_c < \gamma_{cz}$ and $\bar{\gamma}_s^* = \gamma_c$ for $\gamma_c > \gamma_{cz}$, and in αp interactions, $\varepsilon = +1$, and the mean Lorentz factor $\bar{\gamma}_s^*$ is the same as in $p\alpha$ interactions for the same total available energy in the center of mass.

Using equations (4) and (9) with both γ_s^* and γ_m^* replaced by $\bar{\gamma}_s^*$, the laboratory distribution function $F(\gamma, \gamma_s)$ becomes

$$F(\gamma, \gamma_s) = \exp\left[\frac{\varepsilon(\gamma_s - \gamma_c\bar{\gamma}_s^*)}{\cos\Theta_0\sqrt{\gamma_c^2-1}\sqrt{\bar{\gamma}_s^{*2}-1}} - \frac{1}{\cos\Theta_0}\right] \Bigg/ \quad (22)$$

$$\left[\cos\Theta_0\left\{1-\exp(-2/\cos\Theta_0)\right\}\sqrt{\gamma_c^2-1}\sqrt{\bar{\gamma}_s^{*2}-1}\right]$$

In terms of the characteristic energy, E_0, defined above, $\cos\Theta_0$ is given by

$$\cos\Theta_0 = \frac{E_0}{m_p\sqrt{\gamma_c^2-1}\sqrt{\bar{\gamma}_s^{*2}-1}} \quad (23)$$

Since E_o is independent of the incident energy, the energy dependence of $\cos\theta_o$ is determined solely by γ_c and γ_s.

We have also assumed the same distribution function, given by equation (22), for the multibody reactions $n$pd,dd,pt and nHe^3 when pions are produced.

There are no measurements of d, t, or He^3 production by $\alpha\alpha$ reactions. We have assumed arbitrarily that the breakup products of each He^4 nucleus effectively cluster together allowing us to treat the interaction as a two-body process with the two "clusters" having an isotropic angular distribution in the center of mass system. Thus, from equations (4) through (9), with $m_i = m_t = m_s = m_r$, we derive the distribution function for d, t, and He^3 produced in $\alpha\alpha$ reactions with and without pion production to be:

$$F(\gamma,\gamma_s) = \frac{1}{\gamma - 1} \qquad (24)$$

The measurements of Bailey (1956) of the spectra of deuterons and helium-3 produced by 190 Mev protons on carbon are shown in Figure (8), normalized for unit integral. As can be seen these spectra have the same form as those shown in Figure (7), and can also be fitted by an exponential characterized by $1/E_o = 0.14$ (Mev/nucleon)$^{-1}$. Assuming that the triton distribution also has this form and that E_o is independent of incident energy, the d, t, and He^3 distributions for pCNO reactions are the same as those given by equations (22) and (23).

Production Spectra

The rate of production per gram of interstellar material of deuterons and helium-3 nuclei as a function of secondary kinetic energy per nucleon can now be calculated by using the demodulated cosmic ray spectra, production cross-sections and the secondary energy distributions discussed above. We have performed these calculations for a variety of modulating parameters η and R_0 and in general the absolute production increases with increasing η , but is quite insensitive to variations in R_0. The relative contribution of the various production reactions, however, is not strongly dependent on the assumed modulating parameters. For illustration, we show in Figures (9) and (10) the deuteron and helium-3 production spectra, respectively, for η = 350 Mv and R_0 = 0. As can be seen from Figure (9), deuterons of energies less than about 70 Mev/nucleon are produced with equal probability by cosmic-ray helium-4 on hydrogen in the pickup reaction $H(He^4,d)He^3$ and by cosmic ray protons in the multibody breakup of helium; deuterons in the energy range from about 70 to 200 Mev/nucleon are produced mainly in the $(\frac{3}{2},\frac{3}{2})$ resonance reaction of cosmic-ray protons on hydrogen, $H(p,d)\pi^+$; and deuterons of energy greater than about 200 Mev/nucleon are produced with roughly equal probability by the multibody breakup reactions of cosmic-ray helium-4 on hydrogen. It should also be noted that the $\alpha\alpha$ reactions, under the assumptions made above, contribute approximately 20% of the total deuteron production at all energies, and, because

of the lack of experimental data on the cross-sections and kinematics of these reactions, an uncertainty of this order is introduced in the calculation from this source alone.

From Figure (10) we also see that helium-3 nuclei of energies less than about 40 Mev/nucleon are produced principally by cosmic-ray helium-4 on hydrogen in the pickup reaction $H(He^4, He^3)d$, as are the low energy deuterons, while helium-3 nuclei of higher energies are produced predominantly by the breakup of cosmic-ray helium-4 in the reaction $H(He^4, t)2p$, the tritium decaying to helium-3. The $\alpha\alpha$ reactions also produce about 20% of the helium-3 and introduce a corresponding uncertainty in the total production.

III.   DEUTERON AND HELIUM-3 FLUXES AT THE EARTH

From the deuterium and helium-3 production rates in the
interstellar medium, calculated above, we may now determine the
equilibrium density of these secondaries in the galaxy and then,
taking into account modulation, the flux of the d and He^3 nuclei
at the earth.   The equilibrium densities of these nuclei in
the galaxy can be obtained by solving a steady-state continuity
equation in energy space which takes into account leakage from
the galaxy, ionization losses and nuclear breakup of the secon-
daries.

$$\frac{u_s}{\tau_L} + \frac{u_s v}{\lambda_d} + \frac{\partial}{\partial E}\left[\frac{dE}{dt} u_s\right] = \rho \, q_s(E)$$

(25)

where u_s is the secondary cosmic-ray equilibrium density; q_s is
the secondary production rate calculated above, per gram of
interstellar material; ρ is the density of interstellar material
in g/cm^3; τ_L is the leakage lifetime from the galaxy; dE/dt
is the rate of energy loss due to ionization; and λ_d/v is the
mean lifetime against nuclear breakup.   The solution of this
equation can be written as

$$u_s(E) = \frac{\rho}{|dE/dt|} \int_E^\infty dE' q(E') \exp\left[-\int_E^{E'} \frac{dE''}{\tau |dE/dt|}\right]$$

(26)

where τ is the effective lifetime against leakage and nuclear
breakup and is given by:

$$\tau = \left(\frac{1}{\tau_L} + \frac{v}{\lambda_d} \right)^{-1} \tag{27}$$

A more general expression for u_S, which under an appropriate simplification reduces to equation (26) given above, can be obtained by introducing a probability distribution per unit time, $P(t)$, such that $P(t)dt$ is the probability that an observed particle (at $t = 0$) was produced at a time t in the past. In terms of this probability, the number of particles of energy in dE around E which were produced in the time interval dt around t, with energies in dE' around E', is given by

$$du_S(E) = \int q(E') \frac{dE'}{dE} P(t) \, dt \tag{28}$$

where the energies E and E', the time interval t and the energy loss rate dE/dt have to satisfy the following relationship:

$$t = \int_E^{E'} \frac{dE''}{|dE/dt|} \tag{29}$$

Equation (28) can be integrated by assuming that the rate of particle production $\rho q(E)$ is time independent. By changing the variable of integration from t to E' we find that the equilibrium density $u_S(E)$ is given by

$$u_s(E) = \frac{\rho}{|dE/dt|} \int_E^\infty dE' \, q(E') \, P\left[\int_E^{E'} \frac{dE''}{|dE/dt|} \right] \tag{30}$$

Equation (30) is similar to equation (26) given above, except that the exponential distribution is replaced by the more general expression, $P(t)$. The functional form of this expression, however, depends on a variety of factors such as the spatial distribution of the sources, the nature of particle propagation from the sources to the earth, and the properties of the trapping volume of the particles.

In the present study we have assumed a simple exponential distribution, $P(t) = e^{-t/\tau}$. Such a form is valid for the sudden losses resulting from nuclear breakup and it might be a good approximation to a physical situation in which the sources are uniformly distributed in a trapping volume of radius a, from which cosmic rays escape by diffusion caused by scattering off magnetic irregularities. The leakage lifetime τ_L, mentioned above, may then be written as $\tau_L = a^2/(2\lambda_L v)$ where λ_L is the scattering mean free path. For such an exponential distribution, equation (30) becomes equivalent to equation (26).

We now consider the numerical evaluation of equation (26). The energy loss rate dE/dt due to ionization can be replaced by $\rho v \, dE/dR$, where $R(E)$ are charged particle ranges given by

Barkas and Berger (1964). The deuteron breakup cross-section varies with energy but since we find that the lifetime τ is determined principally by leakage, we have taken it to be a constant of 170 mb which corresponds to the average value over the energy range of 10 to 100 Mev/nucleon (Van Oers, 1963; and Davison et al., 1963). The helium-3 breakup cross section is much smaller yet and hence was neglected. The breakup mean path length, λ_d, is given by $\lambda_d = \left(\sigma_d N_a \rho \right)^{-1}$, where N_a is Avogadro's number.

Introducing a mean path lenght against leakage, $\chi = \rho v \tau_L$ equation (26) can be rewritten as

$$j_s(E) = \frac{dR/dE}{4\pi} \int_E^\infty dE' \, q_s(E') \exp\left[-\int_E^{E'} \left(\frac{1}{\chi} + \sigma_d N_a \right) \frac{dR}{dE} \, dE'' \right] \tag{31}$$

where $j_s(E)$ is the secondary cosmic-ray equilibrium intensity in interstellar space. We have evaluated equation (31) for a variety of production spectra, $q_s(E)$, corresponding to a range of values of the modulating parameters η and R_o, defined above. We have then obtained the d and He^3 intensities at the earth by remodulating the resultant equilibrium spectra in interstellar space with the same modulating function as that used in the demodulation process. The results of these calculations, for $R_o = 0$ and for several values of the mean path length x and the modulating parameter η, are shown in Figures (11) and (12) for deuterons and helium-3 nuclei respectively.

The net effect of the process of demodulation and the sub-

sequent remodulation, described above, is a decrease of the
secondary intensity, because secondaries of a given energy
are produced by primaries of higher energy which are there-
fore less modulated than the secondaries which they produce.
This can be seen in Figures (11) and (12) from a comparison of
curves A and C, for zero modulation and modulation characterized
by η = 0.35 BV. Also shown in Figures (11) and (12), are
measurements at the earth of deuterons and He^3 nuclei. In
comparing these data with our calculations, we first consider
the case of zero residual modulation. As can be seen from
curve A, we find that for a cosmic-ray path length of about
$4g/cm^2$ and zero modulation, the calculated He^3 intensities at
energies greater than about 200 Mev/nucleon are in good agree-
ment with the measured intensities (O'Dell et al, 1966; Biswas
et al, 1967; Dennis et al, 1967). However, we also see that
at lower energies the calculated d and He^3 intensities are much
greater than the measured values (Fan et al, 1966a,b), and we
find that for zero modulation no constant value of x can give
a fit to the data. This strongly suggests that a significant
residual modulation exists at solar minimum. This conclusion
is supported by the observed gradient in the cosmic-ray inten-
sity between the orbits of the earth and Mars (O'Gallagher and
Simpson, 1967; O;Gallagher, 1967).

The rigidity dependence of this residual modulation, however,
is not well known and as discussed above, there are significant
disagreements among the various experimenters as to the energy

dependence of the observed cosmic-ray spatial and temporal variations. According to Jokipii and Coleman (1968), the observed power spectrum of the interplanetary field variations indicate that the function f(R), defined above, can be represented by a power law in R with a varying spectral index, ranging from about -0.5 at low rigidities to -2 at high rigidities. Within the experimental errors, this would be consistent with the modulating function given by equation (2) with R_O of the order of 600 MV. Such a rigidity dependent modulation is indeed demanded by the observed deuteron and helium-3 data. As can be seen from curves A in Figures (11) and (12), the calculated d-to-He^3 ratio at, for example, 50 Mev/nucleon for zero residual modulation is about 1.8, whereas the measured ratio at the same energy per nucleon is perhaps as great as 6. Such a difference could result from a modulation of the form $\exp(-\eta/R\beta)$, as given by equation (2) for $R > R_O$. Since at the same energy per nucleon, deuterons have a higher rigidity and hence are less modulated than He^3 nuclei, such a rigidity dependent modulation would increase the calculated d-to-He^3 ratio. Thus, the comparison of the d and He^3 measurements with curve A suggests not only the necessity of some residual modulation but also that above a rigidity of about 600 MV this modulation is velocity as well as rigidity dependent. Because of this, we wish to suggest that the comparison of future measurements of the d-to-He^3 ratio with the calculations described in the present paper, could determine more accurately the charge

dependence and energy spectrum of the residual solar modulation.

Since the present calculations do not depend on processes occurring below rigidities of about 500 MV we have calculated the d and He^3 spectra at the earth for $R_0 = 0$, and a range of values of x and η, thereby determining the values of these parameters which best fit the observed intensities. Within the experimental uncertainties, we find that the available data on both the deuterons and helium-3 nuclei can be best fitted by an energy-independent path length, $x = 4 \pm 1$ g/cm^2, and a residual modulation of the form $\exp\left(-\eta/R\beta\right)$ characterized by $\eta = 0.35 \pm 0.15$ BV. This can be seen by the best fitting curve C and the limiting curves B and D in Figures (11) and (12).

The d/He and He^3/He ratios derived from the present calculations are shown in Figures (13) and (14). Biswas et al (1966) have recently concluded that the energy dependence of the He^3/He ratio can be accounted for only by an energy-dependent path length. However, as can be seen from this figure, our calculations show that both He^3/He and d/He ratios can be explained by an energy-independent path length distribution coupled with a residual solar modulation, which above about 600 MV is both velocity and rigidity dependent and is of the form $\exp\left(-\eta/R\beta\right)$.

ACKNOWLEDGEMENTS

References

Audouze, J., Epherre, M., and Reeves, H., 1967, Preprint.

Badhwar, G. D., and Daniel, R. R., 1963, Prog. Theor. Phys.,
30, 615.

Badhwar, G. D., and Kaplon, M. F., 1966, J. Geophys. Res., 71,
5175.

Bailey, L. E., 1956, University of California Radiation Lab.,
Berkeley, Calif., Reprint UCRL-3334.

Balasubrahmanyan, V. K., Hagge, D. E., Ludwig, G. H., and
McDonald, F. B., 1966a, Proc. Int. Conf. Cosmic Rays, London,
1, 427.

Balasubrahmanyan, V. K., Hagge, D. E., Ludwig, G. H., and
McDonald, F. B., 1966b, J. Geophys. Res., 71, 1771.

Balasubrahmanyan,V.K.,Boldt,E.,and Palmeira,R.A.R., 1967,
J.Geophys.Res.,72,27.

Baldoni, B., Focardi, S., Hromadnik, H., Monari, L., Saporetti, F.,
Femino, S., Mezzanares, F., Bertolini, E., and Gialanella, G.,
1962, Nuovo Cimento, 26, 1376.

Barashenkov, V. S. and Mal'tsev, V. M., 1966, Dubna Report
R-2784.

Barkas, W. H., and Berger, M. J., 1964, NASA SP-3013.

Benveniste, J., and Cork, B., 1953, Phys. Rev. 89, 422.

Biswas, S., Lavakare, P. J., Ramadurai, S., and Sreenivasan, N.,
1967, Proc. Ind. Acad. Sci., 65, 104.

Biswas, S., Ramadurai, S., and Sreenivasan, N., 1966, T.I.F.R.
Preprint, No. NE66-19.

Biswas, S., Ramadurai, S., and Sreenivasan, N., 1968, Proc.
Tenth Intern. Conf. on Cosmic Rays (in press).

Brun, C., Leforth, M., and Tarrago, X., 1962, J. Phys. Rad., 23,
167.

Bunch, S. M., Forster, H. H., and Kim, C. C., 1964, Nuc. Phys.,
53, 241.

Cairns, D.J., Griffith, T. C., Lush, G. J., Metheringham, A. J.,
and Thomas, R. H., 1964, Nuc. Phys., 60, 369.

Cameron, A. G. W., 1959, Ap. J., 129, 676.

Chapman, K. R., Jones, T. W., Khan, Q. H., McKee, J. S. C., Van der Ray, H. B., and Tanimura, Y., 1964, Phys. Letters, 11, 253.

Comstock, G. M., Fan, C. Y., and Simpson, J. A., 1966, Ap. J., 146.

Crawford, F. S., 1953, University of California Radiation Lab., Berkeley, Calif., Rept. UCRL 1756.

Currie, L. A., 1959, Phys. Rev., 114, 878.

Currie, L. A., Libby, W. F., and Wolfgang, R. L., 1956, Phys. Rev. 101, 1557.

Dahanayake, C., Kaplon, M. F., and Lavakare, P. J., 1964, J. Geophys. Res., 69, 3681.

Davison, M., Hopkins, H. W. K., Lyons, L., and Shaw, D. F., 1963, Phys. Letters, 3, 358.

Dennis, B. R., Badhwar, G. D., Deney, C. L. and Kaplon, M. F., 1967, Bull. Am. Phys. Soc., 12, 583.

Dorman, L. I., 1963, Prog. Elem. Particle and Cosmic Ray Physics, 7, 1.

Durbin, B., Loar, H., and Steinberger, J., 1951, Phys. Rev. 84, 581.

Fan, C. Y., Gloeckler, G., Hsieh, K. C., and Simpson, J. A., 1966a, Phys. Rev. Letters, 16, 813.

Fan, C. Y. Gloeckler, G., and Simpson, J. A., 1966b, Phys. Rev. Letters, 17, 329.

Fickinger, W. J., Pickup, E., Robinson, D. K., and Salant, E. O., 1962, Phys. Rev., 125, 2082.

Fichtel, C. E., and Reames, D. V., 1966, Phys. Rev., 149, 995.

Fields, T. H., Fox, J. G., Kane, J. A., Stallwood, R. A., and Sutton, R. B., 1954, Phys. Rev. 95, 638.

Fireman, E. L., and Rowland, F. S., 1955, Phys. Rev., 97, 780.

Foster, F., and Mulvey, J. H., 1963, Nuovo Cimento, 27, 93.

Freier, P. S., and Waddington, C. J., 1965, J. Geophys. Res., 70, 5753.

Gloeckler, G., and Jokipii, J. R., 1966, Phys. Rev. Letters, 17, 203.

Guzhavin, V. M., Kliger, G. K., Kolganov, V. Z., Lebedev, A. V., Marish, K. S., Prokoshkin, Yu, D., Smolyankin, V. T., Sokolov, A. P., Soroko, L. M., and Wachuang, Tsui, 1964, Zh. Eksp. i Teor. Fiz. 46, 1245.

Hart, E. L., Louttit, R. I., Luers, D., Morris, T. W., Willis, W. J., and Yamamoto, S. S., 1962, Phys. Rev., 126, 747.

Hayakawa, S., Ito, K., and Terashima, Y., 1958, Prog. Theor. Phys., Supp. 6, 1.

Hayakawa, S., Horikawa, N., Kajikawa, R., Kikuchi, K., Kobayakawa, H., Matsuda, K., Nagata, S., and Sumi, Y., 1964, Phys. Letters, 8, 330.

Hofmann, D. J., and Winckler, J. R., 1966, Phys. Rev. Letters, 16, 109.

Honda, M., and Lal, D., 1960, Phys. Rev., 118, 1618.

Innes, W. H., 1957, Lawrence Radiation Lab., Berkeley, Calif., Rept. UCRL-8040.

Jokipii, J. R., 1966, Ap. J., 146, 480.

Jokipii, J. R., 1968, Proc. Tenth Intern. Conf. on Cosmic Rays, (in press).

Jokipii, J. R., Coleman, P. J., 1968, J. Geophys. Res. (in press).

Kavaloski, C. D., Bassani, G., Hintz, N. M., 1963, Phys. Rev., 132, 813.

Kozadaev, M. S., Kulyukin, M. M., Sulyaev, R. M., Filippov, A. I., Shcherbakov, Yu. A., 1960, Zh. Eksp. i Teor. Fiz., 38, 708.

Kuzhevskii, B. M., 1966, Yader. Fiz., 4, 130.

Legg, J. C., 1963, Phys. Rev., 129, 272.

Meyer, J. P., Hagge, D. E., and McDonald, F. B., 1968, Proc. Tenth Intern. Conf. on Cosmic Rays (in press).

Moulthrop, P. H., 1955, Phys. Rev., 99, 1509.

Nadi, M., and Riad, F., 1964, Nuc. Phys., 50, 33.

Neganov, B. S., and Parfenov, L. B., 1958, Zh. Eksp. i Teor. Fiz., 34, 767.

O'Dell, F. W., Shapiro, N. M., Silberberg, R., and Stiller, B., 1966, Proc. Int. Conf. on Cosmic Rays, London, 1, 412.

O'Gallagher, J., and Simpson, J. A., 1967, Ap. J., 147, 819.

O'Gallagher, J., 1967, Ap. J., 150, 675.

Ormes, J. F., and Webber, W. R., 1966, Proc. Int. Conf. Cosmic Rays, London, 1, 349.

Parker, E. N., 1958, Phys. Rev., 110, 1445.

Pickup, E., Robinson, D. K., and Salant, E. O., 1962, Phys. Rev., 125, 2091.

Ramaty, R., and Lingenfelter, R. E., 1968, Proc. Tenth Intern. Conf. on Cosmic Rays (in press).

Riddiford, L., Williams, A. W., 1960, Proc. Roy. Soc. London, A257, 316.

Rosenfeld, A. H., 1954, Phys. Rev., 96, 139.

Schulz, A. H., 1952, University of California Radiation Lab., Berkeley, Calif., Rept. UCRL 1756.

Schwarzschild, A., and Zupancic, C., 1963, Phys. Rev., 129, 854.

Selove, W., and Teem, J. M., 1958, Phys. Rev., 112, 1658.

Shapiro, M. M., and Silberberg, R., 1968, Proc. Tenth Intern. Conf. on Cosmic Rays (in press).

Smith, G. A., Courant, A. H., Fowler, E. C., Kraybill, H., Sandweiss, J., and Taft, H., 1961, Phys. Rev., 123, 2160.

Smith, W. R., and Ivash, E. V., 1962, Phys. Rev., 128, 1175.

Stadler, H. L., 1954, Phys. Rev., 96, 496.

Stevenson, M. L., 1953, University of California Radiation Lab., Berkeley, Calif., Rept. UCRL 2188.

Suess, H. E., and Urey, H. C., 1956, Rev. Mod. Phys., 28, 53.

Tannenwald, P. O., 1953, Phys. Rev., 89, 508.

Van Oers, W. T. H., 1963, Thesis. University of Amsterdam.

Waddington, C. J. and Freier, P. S., 1966, Proc. Int. Conf. on Cosmic Rays, London, 1, 345.

Wickersham, A. F., 1957, Phys. Rev., 107, 1050.

FIGURE CAPTIONS

1. Deuteron production cross-section for the reaction
    $H^1(p,d)\pi^+$.

2. Deuteron, triton and helium-3 production cross-sections
    for pHe^4 reactions.

3. Deuteron, triton and helium-3 production cross-sections
    for pCNO reactions.

4. Ranges of the Lorentz factors of the center of mass, and
    of the secondary particle in the center of mass, γ_c and γ_s^*
    respectively, which for the indicated reactions can con-
    tribute to given secondary laboratory Lorentz factors, γ_s.
    The solid lines define the ranges of γ_c and γ_s^* which
    satisfy the inequalities (10), and the dashed lines re-
    present γ_m^* as a function of γ_c.

5. Ranges of the incident kinetic energies per nucleon which
    can contribute to a given secondary energy for the indi-
    cated deuteron producing reactions. These ranges are de-
    termined from the requirements that $\cos\theta^* \leq 1$ and that
    the deuteron Lorentz factor in the center of mass be less
    than or equal to its maximum value determined from the con-
    servation of energy and momentum.

6. Angular distribution in the center of mass of deuterons
    from the reaction $He^4(p,d)He^3$ for various incident proton
    energies.

7. Energy distribution in the laboratory frame of deuterons and tritons from the multibody breakup of He^4.

8. Energy distributions in the laboratory frame of deuterons and helium-3 nuclei from proton-carbon interactions.

9. Deuteron production spectra per gram of interstellar material for the various modes shown in Table I. These spectra were computed for a demodulated cosmic ray intensity with $\eta = 350$ MV and $R_O = 0$.

10. Helium-3 production spectra per gram of interstellar material for the various modes shown in Table I. These spectra were computed for a demodulated cosmic ray intensity with $\eta = 350$ MV and $R_o = 0$.

11. The observed intensity of deuterons, together with the calculated deuteron intensities at the earth for various values of interstellar path lengths and modulating parameters.

12. The observed intensity of helium-3 nuclei, together with the calculated helium-3 intensities at the earth for various values of interstellar path lengths and modulating parameters.

13. The observed ratio of deuterons to helium nuclei, together with the calculated d-to-He ratios at the earth for various values of interstellar path lengths and modulating parameters.

14. The observed ratio of helium-3 to helium nuclei, together with the calculated He^3-to-He ratios at the earth for various values of interstellar path lengths and modulating parameters.

TABLE I

DEUTERON PRODUCTION

1. $p + H^1 \rightarrow d + \pi^+$

2. $p + He^4 \rightarrow d + He^3 + (\pi)$

3. $\alpha + H^1 \rightarrow d + He^3 + (\pi)$

4. $p + He^4 \rightarrow d + 2p + n + (\pi)$

5. $\alpha + H^1 \rightarrow d + 2p + n + (\pi)$

6. $\alpha + He^4 \rightarrow d + p + n + \alpha + (\pi)$

7. $p + He^4 \rightarrow 2d + p + (\pi)$

8. $\alpha + He^1 \rightarrow 2d + p + (\pi)$

9. $\alpha + He^4 \rightarrow 2d + \alpha + (\pi)$

10. $p + CNO \rightarrow d + \ldots + (\pi)$

11. $CNO + H^1 \rightarrow d + \ldots + (\pi)$

HELIUM-3 PRODUCTION

1. $p + He^4 \rightarrow He^3 + d + (\pi)$

2. $\alpha + H^1 \rightarrow He^3 + d + (\pi)$

3. $p + He^4 \rightarrow t + 2p + (\pi)$

4. $\alpha + H^1 \rightarrow t + 2p + (\pi)$

5. $\alpha + He^4 \rightarrow t + p + \alpha + (\pi)$

6. $p + He^4 \rightarrow He^3 + p + n + (\pi)$

7. $\alpha + H^1 \rightarrow He^3 + p + n + (\pi)$

8. $\alpha + He^4 \rightarrow He^3 + n + \alpha + (\pi)$

9. $p + CNO \rightarrow He^3 + \ldots + (\pi)$

10. $CNO + H^1 \rightarrow He^3 + \ldots + (\pi)$

TABLE II

Kinetic Energy (Mev/nucleon)

d producing reactions	E_{th}	E_z	E_{min}	$E_S(th)$	$E_S(min)$	$E_S(\infty)$
$pp \rightarrow d\,\pi^+$	286.5	—	312.4	69.1	63.9	234.1
$p\alpha \rightarrow d\,He^3$	23.0	27.7	—	0.9	—	230.2
$\alpha p \rightarrow d\,He^3$	23.0	—	37.3	14.6	9.1	234.1
$p\alpha \rightarrow d\,2pn$	31.7	38.2	—	1.3	—	230.2
$\alpha p \rightarrow d\,2pn$	31.7	—	51.6	20.1	12.5	234.1
$p\alpha \rightarrow dd\,p$	29.9	36.1	—	1.2	—	230.2
$\alpha p \rightarrow dd\,p$	29.9	—	48.6	19.0	11.8	234.1
$p\,O^{16} \rightarrow d\ldots$	14.3	14.4	—	0.1	—	2847.9
$O^{16}\,p \rightarrow d\ldots$	14.3	—	27.1	12.6	6.6	234.1

He³ producing reactions	E_{th}	E_z	E_{min}	$E_S(th)$	$E_S(min)$	$E_S(\infty)$
$p\alpha \rightarrow He^3\,d$	23.0	37.3	—	0.9	—	37.8
$\alpha p \rightarrow He^3\,d$	23.0	—	27.7	14.6	12.2	622.8
$p\alpha \rightarrow t\,2p$	24.8	40.2	—	1.0	—	37.8
$\alpha p \rightarrow t\,2p$	24.8	—	29.9	15.8	13.1	622.8
$p\alpha \rightarrow He^3\,pn$	24.8	40.2	—	1.0	—	37.8
$\alpha p \rightarrow He^3\,pn$	24.8	—	29.9	15.8	13.1	622.8
$p\,O^{16} \rightarrow \{t\ldots$	16.2	16.4	—	0.1	--	1639.0
$\qquad \{He^3\ldots$	16.2	16.4	—	0.1	--	1639.0
$O^{16}\,p \rightarrow \{t\ldots$	16.2	--	23.0	14.3	10.1	622.8
$\qquad \{He^3\ldots$	16.2	--	23.0	14.3	10.1	622.8

$pp \rightarrow d\pi^{+} \cdots$

KINETIC ENERGY (Bev)

σ (mb)

Figure 1

Figure 2

Figure 3

KINETIC ENERGY/NUCLEON

σ (mb)

p <CNO>

d

He^3

t

Nadi and Riad (1964) and Legg (1963)
Kavaloski, et al (1963)
Bailey (1956) and Fraenkel
(Personal Communication)
Schwarzschild and Zupančič (1963)
Cherny and Pehl (Pers. Comm.)
Honda and Lal (1960)
Currie, et al (1956)
Fireman and Rowland (1955)
Currie (1959)

10 Mev.   100 Mev.   1 Bev.   10 Bev.

1000   100   10   1

Figure 4

Figure 5

He^4(p,d)He^3

31 Mev • Bunch, et al (1964)
55 Mev ▽ Hayakawa, et al (1964)
95 Mev ○ Selove and Teem (1958)

Figure 6

DEUTERON KINETIC ENERGY, E_d (Mev/Nucleon)

$He^4(n,n')$ npd

▼ Innes (1957)
E = 300 Mev

exp{−0.063 E_d}

$He^4(n,n')$ pt

Tannenwald (1953)
E = 90 Mev

Innes (1957)
E = 300 Mev

exp{−0.27 E_t}

TRITON KINETIC ENERGY, E_t (Mev/Nucleon)

Figure 7

Figure 8

KINETIC ENERGY (MEV/NUCLEON)   Figure 9

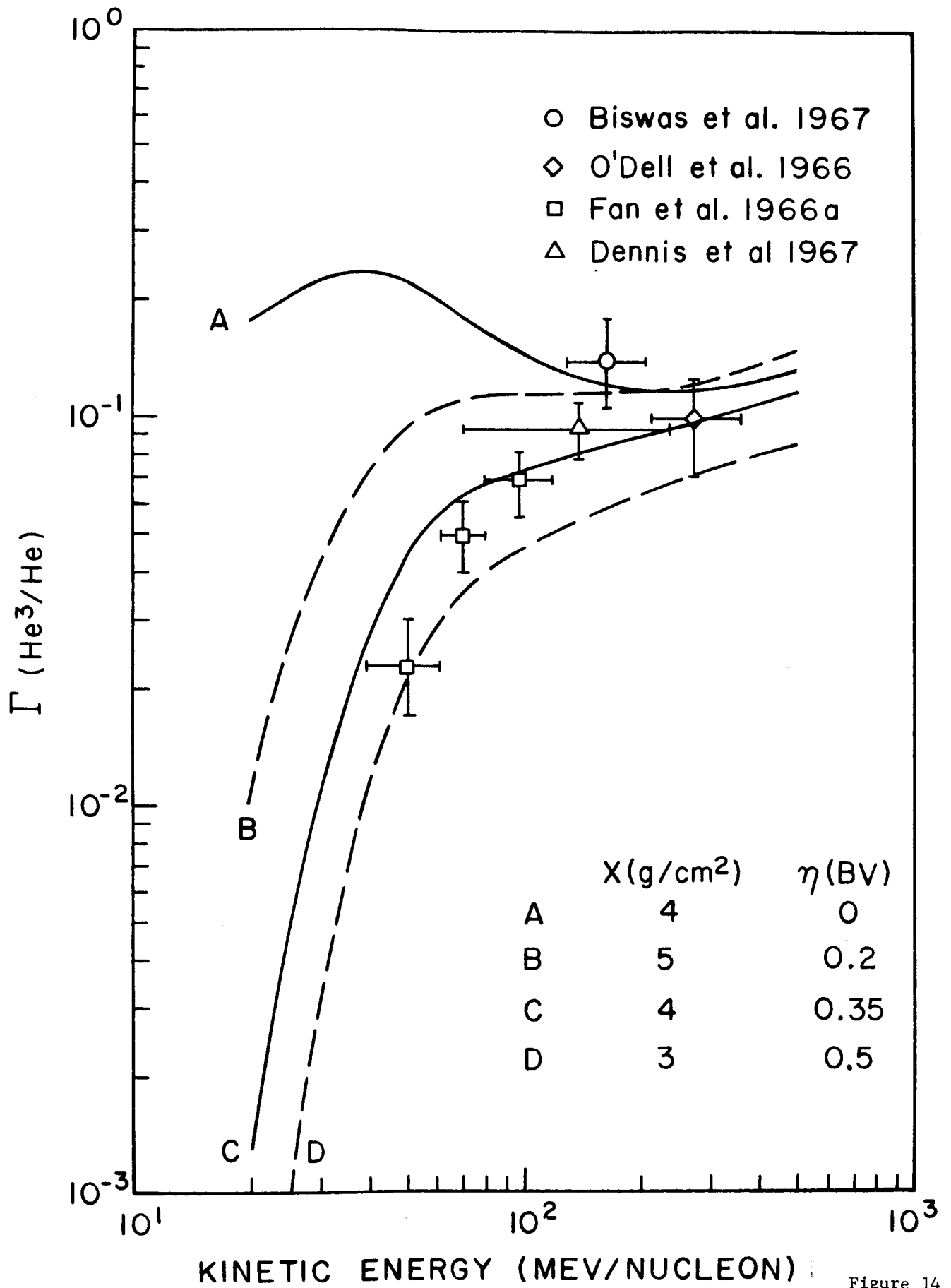HELIUM-3/G·SEC·MEV

TOTAL

KINETIC ENERGY (MEV/NUCLEON)

Figure 10

Figure 11

Figure 12

Figure 13

Figure 14